THE JOURNAL OF BIOLOGICAL CHEMISTRY
Vol. 258, No. 3, Issue of February 10, pp. 1752-1757, 1983
Printed in U.S.A.

The Catalytic Mechanism of Glutathione Reductase as Derived from X-ray Diffraction Analyses of Reaction Intermediates*

(Received for publication, August 30, 1982)

Emil F. Pai‡ and Georg E. Schulz

From the Max-Planck-Institut für medizinische Forschung, D-6900 Heidelberg, Federal Republic of Germany

The mode of binding of NADPH and oxidized glutathione to the flavoenzyme glutathione reductase has been determined by x-ray crystallography. Furthermore, two intermediates of the reaction have been produced in the crystal and have been structurally elucidated. All these analyses were done at 0.3 nm resolution. The results allow the stereochemical description of the mechanism of the enzyme.

The dinucleotide NADPH is bound in an extended conformation with the nicotinamide ring stacking onto the re-face of the flavin part of FAD, and adenine located at the protein surface. The binding of NADPH results in the 2-electron reduced form of the enzyme, EH$_2$. This form has also been analyzed without any ligand bound. In EH$_2$ the redoxactive disulfide bridge of the protein, which lies at the si-face of the flavin ring, is opened and the sulfur of Cys-58 moves by about 0.1 nm into a position where it can attack one of the sulfurs of the substrate oxidized glutathione. This interchange leads to a mixed glutathione-protein disulfide, which can be stabilized in crystals and has been analyzed. By selectively reacting Cys-58 with iodoacetamide the crystalline enzyme can be blocked in its EH$_2$ state. The imidazole of His-467′ is near to all sulfurs taking part in the disulfide bridge exchange and is therefore certainly crucial for catalysis.

The crystallographic results establish that electrons flow from NADPH to the substrate GSSG via flavin and the redoxactive protein disulfide bridge. This is consistent with the scheme that has been postulated from biochemical, spectroscopic, and model studies.

Glutathione reductase (EC 1.6.4.2) is a ubiquitous FAD-containing enzyme (1). It catalyzes the reaction

$$H^+ + NADPH + E \rightleftharpoons NADP^+ + EH_2$$

$$EH_2 + GSSG \rightleftharpoons 2\ GSH,$$

where the intermediate EH$_2$ is the stable 2-electron reduced form of the enzyme. The function of the enzyme is to keep the cellular concentration of the reduced form of glutathione (GSH) high and that of its oxidized form (GSSG) low. Recent publications report a value of about 300:1 for the ratio [GSH]/[GSSG] (2). The enzyme uses NADPH as a source of reduction equivalents. Its substrate GSSG as well as its product GSH are important for a broad range of cellular functions, *e.g.* cell division (3, 4), amino acid transport through membranes (5), regulation of enzymatic activity (6, 7), damage repair (8, 9), drug metabolism (10), and detoxication (11). Moreover, the enzyme has been identified as one of the target molecules of the widely applied antitumor drug carmustine (12, 13).

Glutathione reductase is a member of the family of disulfide reductases. This family also includes lipoamide dehydrogenase and thioredoxin reductase, both FAD-containing redox enzymes that interact with disulfide substrates (1, 14). Lipoamide dehydrogenase especially is very similar to glutathione reductase, both in structural and mechanistic aspects (15, 16). Also the bacterial enzyme mercuric reductase resembles glutathione reductase (17).

In our experiments we used glutathione reductase from human erythrocytes, an enzyme of 2 × 52,400 molecular weight (18, 19). Its amino acid sequence is known (20–23) and has been fitted to an electron density map of 0.2 nm resolution, yielding the complete structure of the molecule (24). Here we report on the crystal structures of the complexes between glutathione reductase and its reaction partners NADPH and GSSG as well as on two reaction intermediates and a covalently modified enzyme. The observed geometries of these complexes and the intermediates allow some conclusions on the mechanism of action of this flavoenzyme.

MATERIALS AND METHODS

Purified glutathione reductase (20) was a gift from Dr. R. H. Schirmer (University of Heidelberg, West Germany). The crystallization of the enzyme has been described earlier (25). Crystals of Form B were transferred to standard storage solutions (26) containing the amount of ligand or reagent stated in Table I. In Soaks A, C, E, and F (Table I) x-ray data were collected from crystals of oxygen-labile enzyme. To prevent reoxidation during the time of data collection, which typically took about a week, these crystals were mounted in quartz capillaries completely filled with the soaking buffer. In these capillaries the crystals were fixed by cotton fibers.

For measuring x-ray reflections we used an automatic four-circle diffractometer ($P2_1$, Syntex Analytical Instruments) modified for protein crystallography (24). Each data set of 0.3 nm resolution was obtained from one single crystal. The procedures of data collection and reduction have been described earlier (24, 27). The binding sites of the substrates were derived from difference-Fourier maps. NADPH has been fitted to its respective map using the interactive display system at Uppsala (28). For placing GSSG we used our own interactive display system.

RESULTS

The exact geometry of the ligands bound to glutathione reductase is given in Fig. 1. The drawing contains the two dinucleotides FAD and NADPH, the substrate GSSG, as well as several amino acid residues which are considered important for catalysis. The positions of the residues and of FAD have been derived from a multi-isomorphous replacement map of 0.2 nm resolution (24). NADPH and GSSG were fitted to difference electron density maps based on Soaks A and B (Table I), respectively. Soak B contained $NADP^+$ in addition

* The costs of publication of this article were defrayed in part by the payment of page charges. This article must therefore be hereby marked "*advertisement*" in accordance with 18 U.S.C. Section 1734 solely to indicate this fact.

‡ Present address, Department of Chemistry, University of California at Santa Barbara, Santa Barbara, CA 93106.

to GSSG. Here the difference density revealed that only the adenosine moiety of oxidized $NADP^+$ is bound to the oxidized enzyme, *E*, whereas from the pyrophosphate onward the nicotinamide moiety is dangling in the solvent.

The intermediate state EH_2 in the catalytic cycle of the enzyme was produced in Soak C. The resulting difference electron density showed one major change as compared to the oxidized enzyme; the disulfide bridge Cys-58:Cys-63 has opened and the sulfur of Cys-58 has moved by about 0.1 nm toward the sulfur of glutathione I. In Fig. 1 these two sulfurs are marked by *dots*. The opening of the disulfide bridge Cys-58:Cys-63 has also been observed in Soak A, where NADPH had reduced the enzyme to its EH_2 form.

The sulfhydryl of Cys-58 created in this reduction is a highly reactive nucleophile and can be rather selectively modified with 2-iodoacetamide to give *E*HR, the blocked 2-electron reduced enzyme. This reaction could be demonstrated for the yeast (29) and the human enzyme (22). In the human enzyme the reaction occurs when NADPH (or dithioerythritol) and 2-iodoacetamide are applied at the same time (22). When we tried a similar procedure on the crystalline human enzyme in Soak D (Table I), the resulting difference-Fourier map showed one significant positive peak with size and shape corresponding to a carboxamidomethyl group plus the displaced sulfur of Cys-58. *E*HR molecules are no longer able to react with glutathione, or, to transfer electrons via FAD to $NADP^+$ in the back reaction. Therefore, crystals of *E*HR are stable in aerobic buffers. So far, we have kept some of them for more than a year without any indications of reoxidation.

In two further experiments, Soaks E and F (Table I), we obtained the mixed disulfide between glutathione I and Cys-58 of the protein. The two difference electron density maps were essentially identical with each other. Glutathione I was bound like the glutathione I moiety of GSSG in Soak B, except for the disulfide bridge which now is glutathione I:Cys-58 instead of glutathione I:glutathione II. The redoxactive disulfide bridge between Cys-58 and Cys-63 is open. The position of glutathione II is occupied at a level of about 20% of glutathione I.

In order to illustrate the gross arrangement of ligands in glutathione reductase we give a structural overview in Fig. 2. The enzyme consists of two subunits, which are related to each other by a 2-fold axis. The subunits are covalently connected by a single disulfide bond across this molecular axis. The 18 NH_2-terminal residues have no defined structure in the crystal. The functional role of this flexible arm is not known. The arm contains a cysteine at position 2. Considering the gross geometry of the enzyme Cys-2 could possibly reach Cys-58 of the redoxactive disulfide bridge. The remaining 460 residues of the polypeptide chain are geometrically organized into four domains. The first two domains along the chain resemble each other structurally and bind FAD and NADPH, respectively. The central and the interface domain follow at the COOH-terminal side.

Considering all residues making up one catalytic center one realizes that they come from five different domains: all four domains of one subunit and the interface domain of the other subunit. As compared to other known protein structures such a large number of domains participating in the catalytic center is unusual. Moreover, the catalytic center lies between subunits. For example both glutathione molecules are stretched between subunits as indicated in Fig. 2.

The catalytic center can be subdivided into two parts, one

TABLE I

Soaking conditions for glutathione reductase crystals

Soak	Ligand or reagent	Conc	Time	pH
A	NADPH	10 mM	30 min	7.0
B	$NADP^+$ and GSSG	10 mM and 10 mM	10 days	7.0
C	2-Mercaptoethanol	1% (w/v)	15 min	7.0
D	Dithioerythritol	2 mM	30 min	7.0
	Dithioerythritol and 2-iodoacetamide	1 mM and 2 mM	150 min	7.0
	$NADP^+$	100 mM	15 min	7.0
	Washing with storage buffer		120 min	7.0
E	2-Mercapthoethanol and GSH	1% (w/v) and 10 mM	5 days	7.0
F	GSH	10 mM	3 days	8.5

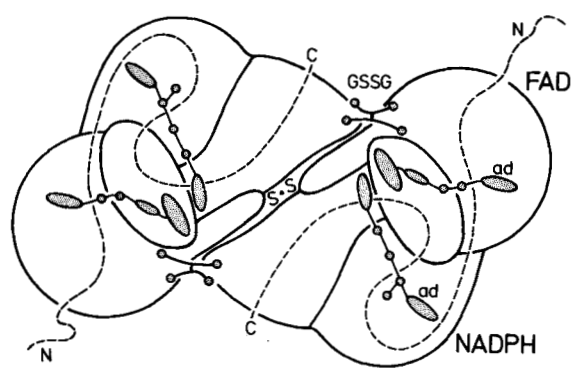

FIG. 2. **Gross structure of the dimeric enzyme glutathione reductase as viewed along the molecular 2-fold axis.** The NH_2-terminal 18 residues are flexible. The remaining polypeptide chain is geometrically organized into four domains. The ligands FAD, NADPH, and GSSG are indicated. There exists a single intersubunit disulfide bridge across the molecular axis.

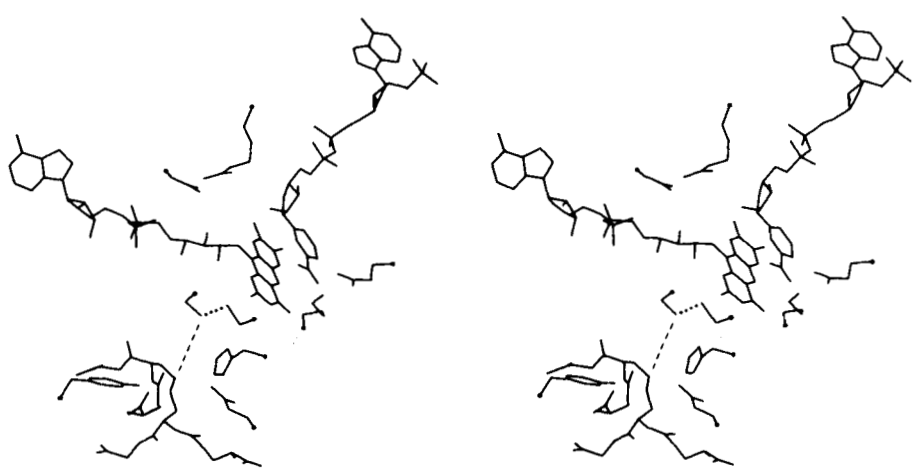

FIG. 1. **Stereo drawing of ligands bound to glutathione reductase together with important amino acid residues.** The positions of FAD, NADPH, and GSSG correspond to those of Fig. 3, where they are named. The same applies for the depicted couples of amino acid side chains Cys-58:Cys-63, Lys-66:Glu-201, Arg-291:Asp-331 and His-467':Glu-472'. The side chain of Tyr-114 is given at its location without GSSG bound. On binding of this substrate the side chain of Tyr-114 moves by about 0.1 nm toward the viewer. All C_α-atoms of these amino acids are marked by *dots*. The bridge Cys-58:Cys-63 is given by a *dotted line*. The formation of the mixed disulfide Cys-58:Glutathione-I is marked by a *dashed line*.

part binding NADPH and the other binding GSSG. This distinction reflects the two-step reaction catalyzed by the enzyme. As shown in Fig. 3 each part corresponds to a deep pocket in the protein, which is filled with solvent when the respective ligand is absent. These two pockets come from opposite sides of a subunit, and meet each other in the subunit center. If these pockets were not separated from each other by flavin and the redoxactive disulfide Cys-58:Cys-63, they would join and form a channel through the subunit. Binding of the substrates to the enzyme in such a geometry results in optimal protection of the reaction center against solvent molecules, which otherwise could interfere with the electron transfer process.

In Fig. 3 we have sketched all those parts of the enzyme-ligand complexes which are given as an exact drawing in Fig. 1. We find it advisable to describe the catalytic center using this sketch and refer the reader to Fig. 1 for exact geometry. The two dinucleotides FAD and NADPH bind in elongated conformations to the protein. The nicotinamide part of NADPH is in close contact with the flavin part of FAD, whereas the adenosine moieties of NADPH and FAD are far apart from each other: the distance between the N1 positions of the two adenines is 2.9 nm.

In the binding pocket of NADPH the side chain of Tyr-197 is indicated by a *dashed line*. Without NADPH being present this phenol ring covers the nicotinamide binding pocket and thus shields flavin against the solvent. On binding of NADPH (Soak A), but not on binding of $NADP^+$ (Soak B), Tyr-197 moves away so that nicotinamide can reach the flavin.

Flavin is surrounded by several pairs of polar, usually ionized residues, which most likely form salt bridges. The most conspicuous one is Lys-66:Glu-201 at the bottom of the nicotinamide binding pocket deeply buried in the protein. The imidazole of His-467′ is fixed by a short and therefore strong hydrogen bond to Glu-472′. This imidazole also contacts the sulfur of the distal Cys-58 and the sulfur of glutathione I. The guanidinium group of Arg-291 is close to the C8α methyl group of flavin. It interacts with Asp-331 via a trapped water molecule. In all three cases, it is the basic partner of these couples of polar residues which is closer to the flavin ring.

Between flavin and GSSG there is the redoxactive disulfide Cys-58:Cys-63 of the protein. This disulfide and its catalytic importance have already been detected by chemical means (1, 30) before the x-ray analysis was started. Moreover, on the basis of chemical and spectroscopic data it had been postulated that this disulfide bridge contacts the flavin ring near to its C4a atom (31). This hypothesis is now perfectly confirmed by the x-ray analysis showing the proximal sulfur of Cys-63 between C4a and C10a (see below). On binding of GSSG, Tyr-114 moves by about 0.1 nm as observed in the difference electron density map. Its phenol ring then fits between the glycine moieties of glutathiones I and II with the hydroxyl group contacting the disulfide bridge of GSSG.

In the first part of the catalytic reaction given above the enzyme is reduced to its stable EH_2 form, and NADPH is oxidized to $NADP^+$. From Soak C and the resulting difference density we know that EH_2 contains an open disulfide bridge Cys-58:Cys-63. Moreover, spectroscopic data indicated that there is a charge transfer complex between a thiolate anion of the proximal Cys-63 and the oxidized flavin ring (32, 33). These data together with the now known geometrical arrangement of the reaction partners (Figs. 1 and 3) clearly indicate that the reduction equivalents flow from nicotinamide via flavin to the Cys-58:Cys-63 bridge.

In this sequence the first step is the transfer of reduction equivalents from nicotinamide to flavin while the two rings are stacked onto each other. The exact geometry of the sandwich between nicotinamide and flavin is given in Fig. 4. We estimate the relative accuracy of this picture as about 0.05 nm. In Fig. 4 the flavin ring is assumed to lie in the paper plane. All other atoms are vertically projected onto this plane. Approximately in the same plane are the carbonyl oxygen of His-467′, which forms a short hydrogen bond to N3, the guanidinium group of Arg-291, and the NH_2-terminal end of the α-helix of residues 338–354.

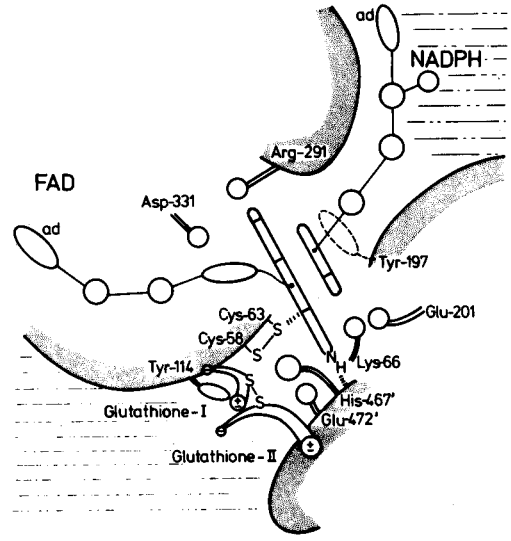

FIG. 3. **The catalytic center of glutathione reductase.** The exact geometry of ligands and amino acid residues is given in Fig. 1, except for Tyr-197, which undergoes a large movement on NADPH binding. The space above and below the catalytic center is filled by protein, so that the binding areas of GSSG and NADPH are deep pockets. The solvent is indicated.

Nicotinamide lies at a distance of 0.34 nm above the paper plane with its ring about parallel to the flavin. The carboxamide side chain is above the pteridin moiety of flavin. The carboxamide seems to be twisted by about 20° as indicated by the *arrow* in Fig. 4. Such a twist fits the observed difference electron density better than a carboxamide coplanar with the pyridine ring, and it allows the amide to form hydrogen bonds of favorable geometry with the carbonyl of Val-370 and the carboxyl of Glu-201, as pointed out in Fig. 4. It should be noted that the twist pushes the carboxamide oxygen onto the center of the pteridin ring of flavin.

The C4′ atom of NADPH is close to N5 of flavin and to the salt bridge Lys-66:Glu-201. The distances are given in Fig. 4. Glutathione reductase belongs to the class of B-specific dehydrogenases (34), which means that the H_S-atom is abstracted from C4′ of NADPH. According to standard geometries this H_S-atom lies at an intermediate level between the rings of flavin and nicotinamide. It is located at approximately equal distance to N5 of flavin and N_ζ of Lys-66. The H_R-atom is placed between C4′ and $O_{\epsilon 1}$ of Glu-201. The observed distance between C4′ and $O_{\epsilon 1}$ is remarkably short.

In Fig. 5 we show the four states of the enzymatic reaction cycle, the geometries of which are known. Since x-ray analyses of proteins do not yield the positions of hydrogen atoms, all hydrogens given in Fig. 5 are guessed. In particular, the ionization states of side chains are unknown. Only the charges of Cys-63 and His-467′ have experimental support (see below).

The oxidized enzyme, E, is represented as State 1 of Fig. 5. Its geometry is known at 0.2 nm resolution (24). The orientation of the imidazole ring of His-467′ is established by the reasonable assumption that one of the nitrogens forms a hydrogen bond to the carboxyl group of Glu-472′. The distances between N_ϵ of His-467′ and the sulfurs of the closed

bridge Cys-58:Cys-63 are given in Table II.

State 2 of the reaction cycle given in Fig. 5 is the complex between $NADP^+$ and EH_2. In our experiments we have produced the complex between NADPH and EH_2 in Soak A because we used a large excess of reduced NADPH and because NADPH binds more tightly to EH_2 than $NADP^+$ (35). In both complexes, however, the NADP conformation and location are essentially the same, because the difference electron density maps of Soak A and of Soak D, where we produced the complex between $NADP^+$ and the blocked reduced enzyme *E*HR (carboxymethylated at Cys-58), correspond closely with each other at 0.3 nm resolution.

The 2-electron reduced form of the enzyme, EH_2, is represented as State 3 of Fig. 5. When compared to State 1, the sulfur of Cys-58 has moved by about 0.1 nm. Furthermore, some positive difference electron density between the proximal sulfur of Cys-63 and flavin appears, indicating a slight movement of the order of 0.01 nm of this sulfur toward flavin on the formation of the charge transfer complex (32, 33). The distances between these two sulfurs and N_ϵ of His-467′ are given in Table II.

In State 4 of Fig. 5 we merged three steps of the reaction, (i) the binding of GSSG to the reduced enzyme EH_2, (ii) the formation of the mixed disulfide between glutathione I and Cys-58 with subsequent release of glutathione II, and (iii) the release of glutathione I. This drawing is based on Soak B, which revealed how GSSG is bound to the oxidized enzyme *E*, and on Soaks E and F, which established that glutathione I forms the mixed disulfide and glutathione II leaves the enzyme first. In the mixed disulfide the sulfurs of glutathione I and Cys-58 are at essentially the same positions as in Soaks B and C, respectively. Although Soaks E and F show a certain although low occupancy of glutathione II the position of sulfur

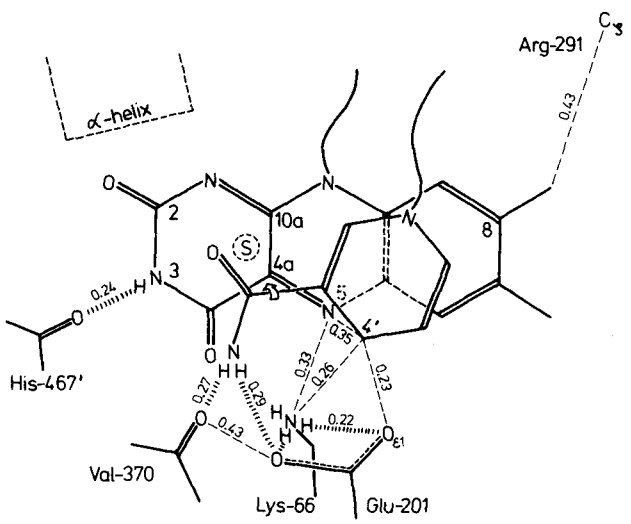

FIG. 4. **Environment of the stacked rings of flavin and nicotinamide.** Flavin is assumed to lie in the paper plane with its re-face pointing to the viewer, all other atoms are projected vertically onto this plane. All distances are given in nanometers. Presumed hydrogen bonds are indicated by *rows of slashes*. Distance measurements are marked by *dashed lines*. Also in the paper plane is the carbonyl oxygen of His-467′ and the center C_ζ of the guanidinium group of Arg-291. The inserted α-helix of residues 338–354 starts close to O2α in the paper plane and extends to the upper rear side. The sulfur *S* is located 0.34 nm below the paper plane and belongs to Cys-63. The nicotinamide ring lies 0.34 nm above the paper plane. Its carboxamide group is twisted as marked. The distance between $O_{\epsilon 2}$ of Glu-201 and N_ζ of Lys-66 is 0.24 nm. The distance between $O_{\epsilon 2}$ and C4′ of nicotinamide is 0.32 nm. The alkyl parts of Lys-66 covers tightly the N5 atom of flavin, the distance between C_ϵ and N5 being 0.34 nm. The accuracy of the nicotinamide position is about 0.05 nm.

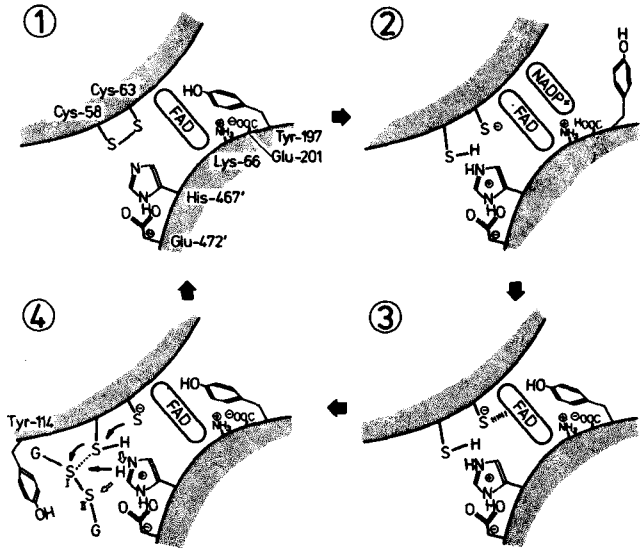

FIG. 5. **Four states of the catalytic reaction cycle of glutathione reductase, for which structural data are available.** State 1 is the oxidized enzyme *E*. State 2 is the complex between $NADP^+$ and the reduced enzyme EH_2. Here, we know the structures of the complexes between NADPH and EH_2 as well as the complex between $NADP^+$ and the blocked (carboxymethylated at Cys-58) reduced enzyme *E*HR. The NADP location in both complexes is very similar. State 3 is the reduced enzyme EH_2, a stable reaction intermediate. In State 4 we combine three catalytic steps, the binding of GSSG to EH_2, the formation of the mixed disulfide between glutathione I and Cys-58 (*dotted line*) with subsequent release of glutathione II, and the release of glutathione I. The *light arrows* refer to assumed hydrogen movements on formation of mixed disulfide and release of glutathione II. The *black arrows* refer to splitting of the mixed disulfide and the release of glutathione I. The hydrogens of all four states are postulated; they cannot be located by x-ray diffraction. For distances see Table II.

TABLE II

Distances between N_ϵ of His-467′ and the sulfurs of Cys-58, Cys-63, and glutathione during the catalytic cycle

The distance errors are about 0.05 nm. Because of its low occupancy, the position of S_{II} in *E*-SG + GSH is not known. Therefore, only a distance limit can be given.

State	Complex	Atoms	Distance
			nm
1	*E*	N_ϵ–S_{58}	0.36
		N_ϵ–S_{63}	0.44
3	EH_2	N_ϵ–S_{58}	0.31
4	*E*·GSSG	S_{58}–S_I	0.50
		N_ϵ–S_I	0.36
		N_ϵ–S_{II}	0.49
4	EH_2·GSSG	S_{58}–S_I	0.36
4	*E*-SG + GSH	N_ϵ–S_I	0.31
		N_ϵ–S_{II}	≧0.38

S_{II} cannot be recognized safely. On formation of the mixed disulfide the sulfur of glutathione II moves away. The distances between the relevant atoms are given in Table II. Assuming that S_{II} moves toward N_ϵ of His-467′ where it can find space, and that it stops at van der Waals distance of 0.32 nm from its former sulfur partner S_I, the resulting distance to N_ϵ amounts to 0.38 nm. Thus, glutathione II may well pick up a proton from His-467′. Moreover, there is no other conspicuous proton donor nearby.

DISCUSSION

Glutathione reductase is catalytically active in the crystals used for x-ray analysis; on addition of NADPH yellow crystals

(State 1 of Fig. 5) turn red (State 3 of Fig. 5), and these red crystals turn yellow again when NADPH is removed and GSSG added. Therefore, the structurally analyzed intermediates are most likely catalytically competent.

The catalytic cycle starts with the binding of NADPH to the oxidized enzyme (State 1 of Fig. 5). As the first intermediate we define State 2 of Fig. 5, where the reduction equivalents have opened the redox-active disulfide bridge. In Soaks A and D (Table I) we produced the complexes $EH_2 \cdot$NADPH and EHR$\cdot$NADP$^+$, which resemble each other closely. Therefore, it is most likely that within the limits of error their geometry corresponds to State 2 of Fig. 5.

The geometric arrangement of nicotinamide, flavin, and their environment are given in Fig. 4. Here, one has to keep in mind that x-ray analyses of proteins do not show hydrogen atoms. As a consequence all hydrogens given in, or discussed in conjunction with Figs. 4 and 5, are either postulated or derived from standard geometries. Fig. 4 demonstrates that the transferred H_S-atom of nicotinamide (34) is near to N5 of flavin and N_ζ of Lys-66. Since N5 is tightly covered by the alkyl part of Lys-66, it is rather unlikely that H_S attaches to N5 and enters the flavin plane. Also, we cannot find any other reasonable pathway for H_S from the re- to the si-face of flavin. Thus, we conclude that H_S does not proceed to the redoxactive disulfide, but eventually remains as a proton in the NADPH-binding pocket (Figs. 3 and 5).

The nature and the sequence of the reduction equivalents transferred from NADPH to flavin and from flavin to the disulfide cannot be directly determined in an x-ray structure analysis. The observed geometry does not rule out previous suggestions (36–40): only the covalent bond between C2′ and C4a proposed by Hemmerich (37) seems to be very unlikely. The atomic arrangement indicates that H_S ends up at N_ζ of Lys-66 after this has pushed one hydrogen over to Glu-201. The short distance between C4′ and $O_{\epsilon 1}$ of Glu-201 may help to drive electrons into flavin.

When immersed in the flavin ring system, the electrons have to be stabilized. A major contribution to this stabilization could come from the presumably positively charged residues around flavin (Fig. 3). Moreover, the NH_2 terminus of α-helix 338–354 is near to N1 and O2α (Fig. 4). This helix stabilizes a negative charge, which occurs in this region in anionic flavin states (41).

For picking up the electrons from flavin the proximal sulfur of Cys-63 may form a short-lived covalent bond to C4a, as has been suggested from spectroscopic data (42). An intermediate bond between sulfur and C4a is likely to occur in the closely related enzyme lipoamide dehydrogenase (31). Moverover, such a bond has been observed in model studies (43, 44). After breaking this bond, Cys-63 forms a thiolate anion. This anion is at the NH_2 terminus of α-helix 63–80 and therefore stabilized by the helix dipole.

In stopped flow experiments the formation of State 2 (Fig. 5) has been resolved into three steps (42). In the light of the then known general geometry at the active center (27), these steps have been interpreted as (i) a charge transfer complex between NADPH (donor) and oxidized flavin (acceptor), (ii) a charge transfer complex between NADP$^+$ (acceptor) and reduced flavin (donor), and (iii) a covalent attachment of the proximal sulfur to C4a (42). The assumed charge transfer complexes, however, do not imply that electrons are passed on via such an interaction.

In the next step of the cycle the enzyme proceeds to State 3 (Fig. 5), the stable intermediate EH_2 that has been characterized in detail (1, 30). EH_2 contains an oxidized flavin and a reduced disulfide. In this step NADP$^+$ leaves its pocket. Presumably, this is facilitated by the surplus positive charge at Lys-66 repelling the positively charged nicotinamide. Furthermore, the additional proton in the salt bridge is released to the solvent via a column of water molecules, and the salt bridge is reinstalled.

As has been shown chemically (1, 30) the enzyme takes up 2 protons from the solvent when proceeding from State 1 to State 3. This happens most likely in the GSSG binding pocket. States 2 is drawn with these protons already present, although nothing is known about the time sequence of NADP$^+$ detachment, salt bridge discharge, and proton uptake. For geometric reasons (Table II) the protons should be picked up one after the other using N_ϵ of His-467′ as a relay station. In EH_2 a hydrogen bond between this N_ϵ and S_{58} is very likely, whereas the distance between N_ϵ and S_{63} is too large for such an interaction. Fig. 5 agrees well with chemical data, showing that a base with a pK of 6.5 has been protonated in EH_2, which indicates that a histidine is involved (45). The charged histidine may also stabilize the thiolate anion.

The reactions from State 1 to State 3 (as well as the complete cycle) lead to a proton release in the NADPH pocket at one side of the enzyme (Fig. 3) and a proton uptake in the GSSG pocket at the other side. As a consequence, the enzyme would perform the function of a proton pump if it were suitably packed into a membrane (46, 47).

The stable intermediate EH_2 allows the subdivision of the reaction cycle into the two parts given above as separate equations. The structure analysis shows that these two parts are also geometrically distinct from each other (Figs. 2, 3, and 5). Between State 1 and State 3 of Fig. 5 the most essential reactions happen at the NADPH site, *i.e.* at the re-face of flavin, whereas the following bridge exchange takes place at the si-face. The degree of separation is also reflected in the observation that transhydrogenase and electron transferase activity, which are by-reactions occurring in the NADPH pocket, are not much affected by enzyme modifications in the GSSG pocket (47).

When the substrate GSSG is bound, the enzyme proceeds to State 4. This figure combines three reaction steps: (i) the binding of GSSG to EH_2, (ii) the formation of the mixed disulfide with subsequent release of glutathione II, and (iii) the release of glutathione I. Our x-ray analysis showed how GSSG is bound to the oxidized enzyme (Soak B). Since the only appreciable difference between EH_2 (State 3) and E (State 1) is the opened disulfide bridge, we can safely use Soaks B and C and derive the structure of the complex $EH_2 \cdot$GSSG from $E \cdot$GSSG and EH_2.

On binding of GSSG, the phenol ring of Tyr-114 moves by about 0.1 nm and accommodates itself snugly between the glycine moieties of glutathione I and II. The tyrosine hydroxyl group is at van der Waals contact to both sulfurs of GSSG (Fig. 5). However, because of its high pK value we hesitate to suggest this hydroxyl as a proton donor for any one of the leaving glutathiones. We do not expect that this pK is lowered in the rather nonpolar environment of the phenol.

From Soaks E and F we know that glutathione I forms a mixed disulfide with the protein, E-SG, and that glutathione II leaves the enzyme first. This order could have been guessed from the structure of $E \cdot$GSSG found with Soak B, because in this complex glutathione I is much more tightly bound than glutathione II. The crystals of Soaks E and F have the red color characteristic for EH_2, indicating that the charge transfer complex between thiolate anion and flavin is still intact. As shown in Table II, the opening of the Cys-58:Cys-63 bridge makes S_{58} move toward S_I (of glutathione I) the distance decreasing from 0.50 to 0.36 nm. At its new position S_{58} can start a nucleophilic attack on S_I while the proton of S_{58} leaves its position between S_{58} and S_{63} and moves towards N_ϵ of His-

467′. Concomitantly, the proton of N_ϵ is handed over to S_{II}, which on breaking of the S_I:S_{II} bond can come as near as 0.38 nm to N_ϵ. Glutathione II is then released.

The new bonding pattern at S_{58} now facilitates a nucleophilic attack from S_{63} onto S_{58}. This leads to the split of the mixed disulfide. Since S_I of this disulfide is close to N_ϵ (Table II), S_I is likely to receive the (second) proton from His-467′. Glutathione I is detached, and His-467′ returns to its unprotonated state. Presumably, the imidazole ring of His-467′ does not move in the catalytic process because it is firmly held by Glu-472′.

The described sequence of events in State 4 of Fig. 5 has already been suggested on the basis of chemical data (1, 29). The structure analyses contribute here by providing rather exact geometric relations and by identifying the reaction partners in GSSG and in the enzyme.

In conclusion we report here the x-ray structures of *E*, complex $EH_2 \cdot NADP^+$ (as inferred from $EHR \cdot NADP^+$ and $EH_2 \cdot NADPH$), EH_2, complex $EH_2 \cdot GSSG$ (as inferred from $E \cdot GSSG$ and EH_2), and *E*-SG, which constitute the steps of the reaction cycle given in Fig. 5. These analyses did not reveal any hydrogens. Therefore, the ionic states of possible charged residues remain unknown. As an exception the thiolate of Cys-58 (32, 33) and the charge of His-467′ in EH_2 (45) have gained some experimental support. In the future we shall try to locate hydrogens by neutron crystallography, which should provide a firmer base for discussing the catalytic mechanism.

Acknowledgment—We thank Dr. R. Heiner Schirmer for providing us with a pure glutathione reductase preparation ready for crystallization as well as for very informative discussions, and Dr. Alwyn Jones for generous help on the interactive display system at Uppsala, Sweden.

REFERENCES

1. Williams, C. H., Jr. (1976) in *The Enzymes* (Boyer, P. D., ed), 3rd ed., Vol. 13, pp. 89–172, Academic Press, New York
2. Akerboom, T. P. M., Bilzer, M., and Sies, H. (1982) *J. Biol. Chem.* **257,** 4248–4252
3. Ii, I., and Sakai, H. (1974) *Biochim. Biophys. Acta* **350,** 151–161
4. Rebhun, L. I., Miller, M., Schnaitmann, T. C., Nath, J., and Mellon, M. (1976) *J. Supramol. Struct.* **5,** 199–219
5. Meister, A. (1981) *Trends Biochem. Sci.* **6,** 231–234
6. Pontremoli, S., and Horecker, B. L. (1970) *Curr. Top. Cell. Regul.* **2,** 173–199
7. Holmgren, A. (1979) *J. Biol. Chem.* **254,** 3672–3678
8. Freedman, R. B. (1979) *FEBS Lett.* **97,** 201–210
9. Kosower, N. S., and Kosower, E. M. (1974) in *Glutathione* (Flohé, L., Benöhr, M. Ch., Sies, H., Waller, H. D., and Wendel, A., eds) pp. 216–227, Georg Thieme Publishers, Stuttgart
10. Carlberg, I., Depierre, J. W., and Mannervik, B. (1981) *Biochim. Biophys. Acta* **677,** 140–145
11. Chasseaud, L. F. (1979) *Adv. Cancer Res.* **30,** 175–274
12. Frischer, H., and Ahmad, R. (1977) *J. Lab. Clin. Med.* **89,** 1081–1091
13. Babson, J. R., and Reed, D. J. (1978) *Biochem. Biophys. Res. Commun.* **83,** 754–762
14. Holmgren, A. (1980) *Experientia (Basel)* Suppl. **36,** 149–180
15. Williams, C. H., Jr., Arscott, L. D., and Schulz, G. E. (1982) *Proc. Natl. Acad. Sci. U. S. A.* **79,** 2199–2201
16. Williams, C. H., Jr., Thorpe, C., and Arscott, L. D. (1978) in *Mechanisms of Oxidizing Enzymes* (Singer, T. P., and Ondarza, R. N., eds) pp. 3–16, Elsevier North-Holland, New York
17. Fox, B., and Walsh, C. T. (1982) *J. Biol. Chem.* **257,** 2498–2503
18. Worthington, D. J., and Rosemeyer, M. A. (1975) *Eur. J. Biochem.* **60,** 459–466
19. Worthington, D. J., and Rosemeyer, M. A. (1976) *Eur. J. Biochem.* **67,** 231–238
20. Krohne-Ehrich, G., Schirmer, R. H., and Untucht-Grau, R. (1977) *Eur. J. Biochem.* **80,** 65–71
21. Schiltz, E., Blatterspiel, R., and Untucht-Grau, R. (1979) *Eur. J. Biochem.* **102,** 269–278
22. Untucht-Grau, R., Schirmer, R. H., Schirmer, I., and Krauth-Siegel, R. L. (1981) *Eur. J. Biochem.* **120,** 407–419
23. Krauth-Siegel, R. L., Blatterspiel, R., Saleh, M., Schiltz, E., Schirmer, R. H., and Untucht-Grau, R. (1982) *Eur. J. Biochem.* **121,** 259–267
24. Thieme, R., Pai, E. F., Schirmer, R. H., and Schulz, G. E. (1981) *J. Mol. Biol.* **152,** 763–782
25. Schulz, G. E., Zappe, H., Worthington, D. J., and Rosemeyer, M. A. (1975) *FEBS Lett.* **54,** 86–88
26. Zappe, H. A., Krohne-Ehrich, G., and Schulz, G. E. (1977) *J. Mol. Biol.* **113,** 141–152
27. Schulz, G. E., Schirmer, R. H., Sachsenheimer, W., and Pai, E. F. (1978) *Nature (Lond.)* **273,** 120–124
28. Jones, T. A. (1978) *J. Appl. Crystallogr.* **11,** 268–272
29. Arscott, L. D., Thorpe, C., and Williams, C. H., Jr. (1981) *Biochemistry* **20,** 1513–1520
30. Massey, V., and Williams, C. H., Jr. (1965) *J. Biol. Chem.* **240,** 4470–4480
31. Thorpe, C., and Williams, C. H., Jr. (1976) *J. Biol. Chem.* **251,** 7726–7728
32. Kosower, E. M. (1966) in *Flavins and Flavoproteins* (Slater, E. C., ed), pp. 1–14, Elsevier, Amsterdam
33. Massey, V., and Ghisla, S. (1974) *Ann. N. Y. Acad. Sci.* **227,** 446–465
34. Stern, B. K., and Vennesland, B. (1960) *J. Biol. Chem.* **235,** 209–212
35. Bulger, J. E., and Brandt, K. G. (1971) *J. Biol. Chem.* **246,** 5578–5587
36. Hamilton, G. A. (1971) in *Progress in Bioorganic Chemistry* (Kaiser, E. T., and Kézdy, T. J., eds) Vol. 1, pp. 83–173 Wiley-Interscience, New York
37. Hemmerich, P. (1976) in *Progress in the Chemistry of Organic Natural Products* (Herz, W., Grisebach, H., and Kirby, G. W., eds) Vol. 33, pp. 451–527, Springer-Verlag, Wien
38. Walsh, C. (1980) *Accts. Chem. Res.* **13,** 148–155
39. Bruice, T. C. (1980) *Am. Chem. Res.* **13,** 256–262
40. Blankenhorn, G. (1976) *Eur. J. Biochem.* **67,** 67–80
41. Müller, F., Hemmerich, P., Ehrenberg, A., Palmer, G., and Massey, V. (1970) *Eur. J. Biochem.* **14,** 185–196
42. Huber, P. W., and Brandt, K. G. (1980) *Biochemistry* **19,** 4568–4575
43. Yokoe, I., and Bruice, T. C. (1975) *J. Am. Chem. Soc.* **97,** 450–451
44. Loechler, E. L., and Hollocher, T. C. (1980) *J. Am. Chem. Soc.* **102,** 7312–7354
45. Matthews, R. G., Ballou, D. P., Thorpe, C., and Williams, C. H., Jr. (1977) *J. Biol. Chem.* **252,** 3199–3207
46. Fritsch, K. G., Pai, E. F., Schirmer, R. H., Schulz, G. E., and Untucht-Grau, R. (1979) *Hoppe-Seylers Z. Physiol. Chem.* **360,** 261–262
47. Mannervik, B., Boggaram, V., Carlberg, I., and Larson, K. (1980) in *Flavins and Flavoproteins* (Yagi, K., and Yamano, T., eds) pp. 173–187, Japan Scientific Societies Press, Tokyo

The catalytic mechanism of glutathione reductase as derived from x-ray diffraction analyses of reaction intermediates.

E F Pai and G E Schulz

J. Biol. Chem. 1983, 258:1752-1757.
